Determination of Phase Composition of MCM-48/ Lamellar Phase Mixtures Using Nitrogen Adsorption and Thermogravimetry

Michal Kruk,[†] Mietek Jaroniec,*[,†] M. Lourdes Peña,[‡] and Fernando Rey[‡]

Department of Chemistry, Kent State University, Kent, Ohio 44240, and Instituto de Tecnologia Quimica (C.S.I.C.−U.P.V.), Avenida de los Naranjos sln, 46022 Valencia, Spain

Received June 5, 2002. Revised Manuscript Received August 5, 2002

It is shown that gas adsorption and thermogravimetry are suitable for the determination of the phase composition of MCM-48/lamellar phase mixtures, which often are formed at different stages of the MCM-48 synthesis. The occurrence of the lamellar phase can be easily detected by analyzing as-synthesized materials by X-ray diffraction (XRD). However, it is not convenient to use this technique to quantify the composition of MCM-48/lamellar mixtures because of the overlap of the characteristic XRD peaks of these two phases and an inherent difficulty in applying the quantitative analysis for materials with amorphous frameworks presenting solely low-angle XRD peaks due to the long-range ordering of the pore arrays. On the other hand, the quantification of the lamellar phase in MCM-48/lamellar mixtures can be readily achieved by fitting the nitrogen adsorption isotherm for the calcined mixed phase with a linear combination of nitrogen adsorption isotherms for pure calcined MCM-48 and pure calcined (collapsed) lamellar phases. When the pure phases are properly selected, a good fit is often achieved in the entire relative pressure range and the sum of fitting coefficients is close to 1. In such a case, the fitting coefficients can be regarded as weight fractions of the pure components in the mixture. A semiquantitative evaluation of the content of the lamellar phase in MCM-48/lamellar mixtures can also be made on the basis of thermogravimetric (TGA) weight change patterns of as-synthesized samples because of a dramatically different weight loss behavior for as-synthesized MCM-48 and lamellar phase. Phase composition estimates from gas adsorption and TGA data were found to be similar. Because of the fact that adsorption and TGA data are often acquired during a routine analysis of surfactant-templated materials, the methods reported in this study can readily be used to assess the phase purity of MCM-48.

Introduction

The MCM-48 silica of cubic *Ia*3*d* symmetry, which was first reported by the Mobil scientists in the early 1990s,[1] has attracted considerable and still growing attention. This is because this material with interconnected three-dimensional (3-D) pore system[2] is a promising catalyst,[3−20] catalyst support,[21] chromatographic packing material,[22,23] immobilization medium,[24,25] and the host[26,27] or template[28−30] for the synthesis of advanced nanostructures. The structure of MCM-48 is now well-understood as a system of two disconnected, enan-

* To whom correspondence should be addressed. E-mail: jaroniec@columbo.kent.edu. Phone: (330)672 3790. Fax: (330)672 3816.
[†] Kent State University.
[‡] C.S.I.C.−U.P.V.

(1) Beck, J. S.; Vartuli, J. C.; Roth, W. J.; Leonowicz, M. E.; Kresge, C. T.; Schmitt, K. D.; Chu, C. T−W.; Olson, D. H.; Sheppard, E. W.; McCullen, S. B.; Higgins, J. B.; Schlenker, J. L. *J. Am. Chem. Soc.* **1992**, *114*, 10834.
(2) Monnier, A.; Schuth, F.; Huo, Q.; Kumar, D.; Margolese, D.; Maxwell, R. S.; Stucky, G. D.; Krishnamurty, M.; Petroff, P.; Firouzi, A.; Janicke, M.; Chmelka, B. F. *Science* **1993**, *261*, 1299.
(3) Zhao, D.; Goldfarb, D. *J. Chem. Soc., Chem. Commun.* **1995**, 875.
(4) Schmidt, R.; Junggreen, H.; Stocker, M. *Chem. Commun.* **1996**, 875.
(5) Koyano, K. A.; Tatsumi, T. *Chem. Commun.* **1996**, 145.
(6) Morey, M.; Davidson, A.; Stucky, G. D. *Microporous Mater.* **1996**, *6*, 99.
(7) Zhang, W. Z.; Pinnavaia, T. J. *Catal. Lett.* **1996**, *38*, 261.
(8) Morey, M.; Davidson, A.; Eckert, H.; Stucky, G. D. *Chem. Mater.* **1996**, *8*, 486.
(9) Ryoo, R.; Jun, S.; Kim, J. M.; Kim, M. J. *Chem. Commun.* **1997**, 2225.
(10) Hartmann, M.; Racouchot, S.; Bischof, C. *Chem. Commun.* **1997**, 2367.
(11) Echchahed, B.; Moen, A.; Nicholson, D.; Bonneviot, L. *Chem. Mater.* **1997**, *9*, 1716.
(12) Kosslick, H.; Lischke, G.; Landmesser, H.; Parlitz, B.; Storek, W.; Fricke, R. *J. Catal.* **1998**, *176*, 102.
(13) Kawi, S.; Te, M. *Catal. Today* **1998**, *44*, 101.
(14) Morey, M. S.; Stucky, G. D.; Schwarz, S.; Froba, M. *J. Phys. Chem. B* **1999**, *103*, 2037.
(15) Morey, M. S.; Bryan, J. D.; Schwarz, S.; Stucky, G. D. *Chem. Mater.* **2000**, *12*, 3435.
(16) Yuan, Z. Y.; Luo, Q.; Liu, J. Q.; Chen, T. H.; Wang, J. Z.; Li, H. X. *Microporous Mesoporous Mater.* **2001**, *42*, 289.
(17) Walker, J. V.; Morey, M.; Carlsson, H.; Davidson, A.; Stucky, G. D.; Butler, A. *J. Am. Chem. Soc.* **1997**, *119*, 6921.
(18) Tatsumi, T.; Koyano, K. A.; Igarashi, N. *Chem. Commun.* **1998**, 325.
(19) Eswaramoorthy, M.; Neeraj; Rao, C. N. R. *Chem. Commun.* **1998**, 615.
(20) Nagl, I.; Widenmeyer, M.; Grasser, S.; Kohler, K.; Anwander, R. *J. Am. Chem. Soc.* **2000**, *122*, 1544.
(21) Froba, M.; Kohn, R.; Bouffaud, G.; Richard, O.; van Tendeloo, G. *Chem. Mater.* **1999**, *11*, 2858.
(22) Thoelen, C.; Van de Walle, K.; Vankelecom, I. F. J.; Jacobs, P. A. *Chem. Commun.* **1999**, 1841.
(23) Gallis, K. W.; Eklund, A. G.; Jull, S. T.; Araujo, J. T.; Moore, J. G.; Landry, C. C. *Stud. Surf. Sci. Catal.* **2000**, *129*, 747.

10.1021/cm020616i CCC: $22.00
Published on Web 09/11/2002

tiomeric networks of mesoporous channels that exhibit three-directional pore branching.[2,31−34] Such a structure is expected to be less prone to the pore blocking than one-dimensional channels such as those in MCM-41 silica,[16,35−38] and it should allow a faster diffusion of the reactants and products through a tridirectional channel structure. It was demonstrated that the MCM-48 framework can be doped with a variety of heteroatoms, such as Mn,[3,9] Al,[4,9,12] Ti,[5−7,17,18] V,[8] Sn,[9] Zn,[9,10] Cu,[10] Fe,[11,12] Ga,[12] Cr,[13] Zr,[14] W,[15] Mo,[15] and B,[16] which provide tunable catalytic properties for the final material. Moreover, the supporting of inorganic species on the MCM-48 surface can be accomplished.[21] The MCM-48 surface can be modified by chemical bonding of organic or organometallic groups,[18,20,22,23] which introduces surface properties useful for instance in liquid chromatography.[22,23] MCM-48 was also found suitable for the immobilization of biomolecules.[24,25] Another highly promising area for the application of MCM-48 is its use as a host for the preparation of silica/metal[27] and silica/polymer[26] composites, and its use as a template for the synthesis of ordered mesoporous carbons,[28] which are prospective high-surface-area periodic adsorbents, and metal networks,[29,30] including chiral platinum networks with crystalline frameworks.[30]

From the overview presented above, it is clear that MCM-48 is highly promising for many applications. In all these applications, the purity of the MCM-48 phase is important because the impurities may introduce undesirable pore size and shape heterogeneity, which is likely to affect transport properties, the extent of useful surface area and pore volume, and the phase purity of MCM-48-templated nanostructures. On the other hand, MCM-48 often is formed as a result of phase transformation from another ordered surfactant-templated phase[35−45] and also usually has a tendency to transform to yet another ordered surfactant-templated phase,[35,36,38,39,42,46,47] the latter being lamellar in most cases. Consistently, the formation of MCM-48 contaminated by other surfactant-templated phases was often observed.[35,36,38,41,43−46,48,49] Under certain conditions, MCM-48 may also become contaminated by an amorphous nonmesostructured silica phase.[33] Because of that, MCM-48 samples are likely to contain impurities, unless special precautions during the synthesis are taken. Therefore, it is important to properly characterize MCM-48 materials during both the synthesis methodology development and the preparation of particular samples intended for applications. An obvious step in the characterization is to acquire an XRD pattern for as-synthesized MCM-48,[35−44,46−49] which allows one to qualitatively determine the presence of ordered impurities, while the acquisition of XRD patterns for calcined samples only would result in the loss of an opportunity to easily detect the contamination with lamellar phase which is unstable upon surfactant removal. However, XRD is in general not particularly suitable for the quantitative phase composition determination for most ordered surfactant-templated materials, such as silicas, because of noncrystallinity of their frameworks.[50] Despite that, some attempts to use XRD for quantitative phase composition analysis of surfactant-template materials have been made.[48,51,52] In particular, the quantitative XRD phase composition determination can be meaningfully achieved by using an internal standard (doping) method, but the procedure is not convenient because of the need for the preparation of pure phases of structural properties highly similar to those of the components of mixed phases and their use to prepare doped samples for the analysis.[53] Also, there are additional difficulties for most of the laboratories to obtain quantitative X-ray data at such low 2θ angles working with conventional lab X-ray diffractometers. Therefore, there is a need to develop other, indirect methods for the quantitative phase composition determination for ordered mesoporous materials, such as those based on NMR,[54,55] gas adsorption,[53,56−59] and thermogravimetry (TGA).[53,59] However, some approaches proposed to achieve this goal are likely to be highly inaccurate, while some others are not convenient in practical applications or were not described in a complete manner. In particular, the phase composition determination should not

(24) Washmon-Kriel, L.; Jimenez, V. L.; Balkus, K. J., Jr. *J. Mol. Catal. B: Enzym.* **2000**, *10*, 453.
(25) Han, Y.-J.; Watson, J. T.; Stucky, G. D.; Butler, A. *J. Mol. Catal. B: Enzym.* **2002**, *17*, 1.
(26) Moller, K.; Bein, T.; Fischer, R. X. *Chem. Mater.* **1998**, *10*, 1841.
(27) Ko, C. H.; Ryoo, R. *Chem. Commun.* **1996**, 2467.
(28) Ryoo, R.; Joo, S. H.; Jun, S. *J. Phys. Chem. B* **1999**, *103*, 7743.
(29) Kang, H.; Jun, Y.-w.; Park, J.-I.; Lee, K.-B.; Cheon, J. *Chem. Mater.* **2000**, *12*, 3530.
(30) Shin, H. J.; Ryoo, R.; Liu, Z.; Terasaki, O. *J. Am. Chem. Soc.* **2001**, *123*, 1246.
(31) Schmidt, R.; Stocker, M.; Akporiaye, D.; Torstad, E. H., Olsen, A. *Microporous Mater.* **1995**, *5*, 1.
(32) Alfredsson, V.; Anderson, M. W. *Chem. Mater.* **1996**, *8*, 1141.
(33) Kim, J. M.; Kim, S. K.; Ryoo, R. *Chem. Commun.* **1998**, 259.
(34) Carlsson, A.; Kaneda, M.; Sakamoto, Y.; Terasaki, O.; Ryoo, R.; Joo, S. H. *J. Electron Microsc.* **1999**, *48*, 795.
(35) Xu, J.; Luan, Z.; He, H.; Zhou, W.; Kevan, L. *Chem. Mater.* **1998**, *10*, 3690.
(36) Pena, M. L.; Kan, Q.; Corma, A.; Rey, F. *Microporous Mesoporous Mater.* **2001**, *44−45*, 9.
(37) Landry, C. C.; Tolbert, S. H.; Gallis, K. W.; Monnier, A.; Stucky, G. D.; Norby, P.; Hanson, J. C. *Chem. Mater.* **2001**, *13*, 1609.
(38) Kim, W. J.; Yoo, J. C.; Hayhurst, D. T. *Microporous Mesoporous Mater.* **2001**, *49*, 125.
(39) Fyfe, C. A.; Fu, G. *J. Am. Chem. Soc.* **1995**, *117*, 9709.
(40) Huo, Q.; Margolese, D. I.; Stucky, G. D. *Chem. Mater.* **1996**, *8*, 1147.
(41) Gallis, K. W.; Landry, C. C. *Chem. Mater.* **1997**, *9*, 2035.
(42) Ryoo, R.; Kim, J. M. In *Proceedings of the 12th International Zeolite Conference*; Treacy, M. M. J., Marcus, B. K., Bisher, M. E., Higgins, J. B., Eds.; Materials Research Society: Pittsburgh, 1999; p 689.
(43) Sayari, A. *J. Am. Chem. Soc.* **2000**, *122*, 6504.
(44) Tolbert, S. H.; Landry, C. C.; Stucky, G. D.; Chmelka, B. F.; Norby, P.; Hanson, J. C.; Monnier, A. *Chem. Mater.* **2001**, *13*, 2247.
(45) Liu, Y.; Karkamkar, A.; Pinnavaia, T. J. *Chem. Commun.* **2001**, 1822.
(46) Corma, A.; Kan, Q.; Rey, F. *Chem. Commun.* **1998**, 579.
(47) Ryoo, R.; Joo, S. H.; Kim, J. M. *J. Phys. Chem. B* **1999**, *103*, 7435.
(48) Romero, A. A.; Alba, M. D.; Zhou, W.; Klinowski, J. *J. Phys. Chem. B* **1997**, *101*, 5294.
(49) Yang, Y.; Belfares, L.; Larachi, F.; Grandjean, B. P. A.; Sayari, A. *Stud. Surf. Sci. Catal.* **2000**, *129*, 871.
(50) Ciesla, U.; Schuth, F. *Microporous Mesoporous Mater.* **1999**, *27*, 131.
(51) Cheng, C.-F.; Park, D. H.; Klinowski, J.*J. Chem. Soc., Faraday Trans.* **1997**, *93*, 193.
(52) Neeraj; Rao, C. N. R. *J. Mater. Chem.* **1998**, *8*, 1631.
(53) Kruk, M.; Jaroniec, M.; Yang, Y.; Sayari, A. *J. Phys. Chem. B* **2000**, *104*, 1581.
(54) Firouzi, A.; Atef, F.; Oertli, A. G.; Stucky, G. D.; Chmelka, B. F. *J. Am. Chem. Soc.* **1997**, *119*, 3596.
(55) Wang, L.-Q.; Exarhos, G. J.; Liu, J. *Adv. Mater.* **1999**, *11*, 1331.
(56) Ortlam, A.; Rathousky, J.; Schulz-Ekloff, G.; Zukal, A. *Microporous Mater.* **1996**, *6*, 171.
(57) Schulz-Ekloff, G.; Rathousky, J.; Zukal, A. *Microporous Mesoporous Mater.* **1999**, *27*, 273.
(58) Kruk, M.; Jaroniec, M.; Sayari, A. *Chem. Mater.* **1999**, *11*, 492.
(59) Kruk, M.; Jaroniec, M.; Yang, Y.; Sayari, A. *Stud. Surf. Sci. Catal.* **2000**, *129*, 577.

be based on such quantities as specific surface area, pore volume (both available from gas adsorption data), and surfactant content (for instance, from TGA), simply because these properties can vary widely for phase-pure ordered materials of the same structural type.[60,61] Even the method for surfactant removal may influence the obtained specific surface area and pore volume. The surfactant content for a material with a given structure templated by the same surfactant is dependent on the synthesis conditions, and moreover different kinds of impurities may result in negative or positive deviations from the content characteristic for a pure phase synthesized under particular conditions. On the other hand, one of the hitherto proposed phase composition quantification methods based on NMR is not particularly convenient because of the requirement of the use of a deuterated surfactant template,[54] while the other method free from such constraints was only briefly mentioned without the actual demonstration of its feasibility.[55]

It has recently been demonstrated that unambiguous and reliable quantitative phase composition determination for MCM-41/lamellar phase mixtures can be achieved simply by fitting an adsorption isotherm for a calcined mixed phase material with a linear combination of adsorption isotherms for the pure components.[53] In this work, pure phases (MCM-41 and lamellar phase), which were purposefully synthesized, exhibited properties very similar to those of the components of the mixed phases, and consequently, remarkably good fits were obtained in the entire pressure range and the fitting coefficients obtained provided weight fractions of the components in the mixture. The adsorption-based quantification of phase composition was possible in this case because of markedly different adsorption properties of calcined MCM-41 and calcined (collapsed) lamellar phases. This approach was further generalized by using an empirical modeling to generate adsorption isotherms for MCM-41 components of arbitrarily chosen pore size, thus eliminating the need for experimental adsorption data for MCM-41 with the pore diameter close to that for the component of the mixed phase. In addition, a semiquantitative phase composition determination from thermogravimetric weight-change curves was also possible for as-synthesized MCM-41/lamellar phase mixtures because of the fact that the lamellar phase exhibits a prominent weight loss (related to surfactant decomposition) at temperatures below those in which a major weight loss for the MCM-41 phase takes place.[53] These phase composition estimates from adsorption, and TGA, as well as the ones from quantitative XRD (the doping method) were consistent.

Herein, the quantitative analysis of phase composition from nitrogen adsorption isotherms is extended on MCM-48/lamellar mixtures, whose proper characterization is important from the point of view of MCM-48 synthesis and applications. It is further demonstrated that semiquantitative phase composition determination can also be accomplished in this case simply using TGA. In both cases, the analysis requires the knowledge of gas adsorption isotherms and weight change patterns for pure phases of structures similar to those of the components of the mixed phases. However, once the required data for pure phases are collected, the phase composition for a mixed phase can be determined on the basis of data from a single gas adsorption or TGA measurement.

Table 1. Synthesis Conditions of the Samples Studied in This Work

sample	*x*	*y*	*z*	temp (K)	time (days)
V1	0.28	0	45	423	1
VL1	0.33	0	100	423	1
VL2	0.30	0	39	408	14
VL3	0.39	0	39	423	1
VL4	0.35	0.05	39	423	1
L1	0.35	0	39	423	2
L2	0.35	0	39	423	5
L3	0.35	0	39	423	7

Experimental Section

Materials. Pure MCM-48 (herein referred to as V1; the notation of the MCM-48 and lamellar phases as V and L is adopted from ref 39) and lamellar phases (denoted L1−L3) as well as MCM-48/lamellar mixtures (denoted VL1-VL4) were synthesized as described elsewhere.[36] The synthesis gel has the following molar composition:

$$SiO_2{:}x\text{CTAOH}{:}y\text{CTABr}{:}zH_2O$$

where CTABr is hexadecyltrimethylammonium bromide (Aldrich) and CTAOH is a hexadecyltrimethylammonium hydroxide that was obtained by double anionic exchange using a hydroxide form of the anionic DOWEX SBR resin (Aldrich). The silicon source was an amorphous silica (Aerosil-200 from Degussa). Typically, the crystallization was performed at 423 K (except for sample VL2, for which the crystallization was carried out at 408 K) in Teflon-lined stainless steel autoclaves for different periods of time. The solids were recovered by filtration, exhaustively washed with distilled water, and finally dried at 333 K overnight. The exact values of *x*, *y*, *z*, temperature, and time of crystallization were chosen to obtain different ratios of cubic to lamellar phases in the samples. The exact synthesis conditions for each sample are given in Table 1.

C16−MCM-48 and C14−MCM-48 samples used for comparison were reported in refs 62 and 63 and denoted V(ref 62) and V(ref 63), respectively. C14− and C16−MCM-41 silicas were described in ref 64 and are denoted H1 (ref 64) and H2 (ref 64), respectively. Pure lamellar phase referred to as L (ref 53) was reported in ref 53.

Measurements. XRD patterns were acquired using Cu Kα radiation on a Phillips X'Pert MPD diffractometer equipped with a PW3050 goniometer using secondary monochromated Cu Kα radiation. Nitrogen adsorption isotherms were measured on a Micromeritics ASAP 2010 volumetric adsorption analyzer. Before the measurements, the samples were outgassed for 2 h at 473 K in the port of the adsorption analyzer. Weight change curves were recorded under a nitrogen atmosphere on a TA Instruments TGA 2950 high-resolution thermogravimeter in the high-resolution mode with a maximum heating rate of 5 K min^{-1}. About 10 mg of as-synthesized sample was used for each TGA run. Elemental analyses of the as-prepared materials were carried out on a Carlo Erba 1106 instrument.

Calculation Procedures. The BET specific surface area[65] was calculated from the nitrogen adsorption data in the

(60) Di Renzo, F.; Coustel, N.; Mendiboure, M.; Cambon, H.; Fajula, F. *Stud. Surf. Sci. Catal.* **1997**, *105*, 69.
(61) Sayari, A. Liu, P.; Kruk, M.; Jaroniec, M. *Chem. Mater.* **1997**, *9*, 2499.
(62) Kruk, M.; Jaroniec, M.; Ryoo, R.; Kim, J. M. *Chem. Mater.* **1999**, *11*, 2568.
(63) Kruk, M.; Jaroniec, M.; Ryoo, R.; Joo, S. H. *Chem. Mater.* **2000**, *12*, 1414.
(64) Kruk, M.; Jaroniec, M.; Sakamoto, Y.; Terasaki, O.; Ryoo, R.; Ko, C. H. *J. Phys. Chem. B* **2000**, *104*, 292.

relative pressure range from 0.04 to 0.2. The total pore volume[65] was estimated from the amount adsorbed at a relative pressure of about 0.99. The external surface area and the sum of the primary mesopore volume and micropore volume were evaluated using the α_s plot method[65,66] in the α_s range from 1.8 to 2.2. The standard reduced adsorption α_s for reference adsorbent is defined as an amount adsorbed at a given pressure divided by the amount adsorbed at a relative pressure of 0.4. Herein, the primary mesopore volume is defined as a sum of the volume of primary (ordered) mesopores of MCM-48 and the volume of disordered mesopores of the calcined lamellar phase. The micropore volume was qualitatively estimated using the α_s plot method from the data in the α_s range from 0.4 to 0.7. This estimation may be somewhat inaccurate because pores in the calcined (collapsed) lamellar phase exhibit a very broad size distribution and therefore some of them are likely to exhibit pore filling at pressures corresponding to the 0.4−0.7 α_s range, which is expected to lead to some underestimation of the micropore volume. The pore size distribution was calculated using the Kruk−Jaroniec−Sayari (KJS) method,[67] which employs the Barrett−Joyner−Halenda algorithm and the pore diameter−capillary condensation pressure relation derived using a series of MCM-41 silicas as model adsorbents.[67] The reference adsorption isotherm used in the α_s plot analysis and the statistical film thickness curve suitable for the use in the KJS method are based on the nitrogen adsorption isotherm on a macroporous silica gel and were reported in ref 66. The degree of primary mesopore filling was calculated by subtracting the adsorption on the external surface from the experimental adsorption isotherm data (as described in ref 67) and dividing the obtained adsorption isotherm for ordered mesopores by the maximum amount adsorbed in the ordered mesopores (assessed using the α_s plot method).

Results and Discussion

It has been proposed that the mesophase transformations of nanostructured silica/surfactant materials can be understood by considering the interplay between the organic packing,[36,44,68−70] the interfacial charge matching between the positively charged headgroups of the surfactant and the negatively charged silica layer.[36,44,70] Also, it has been found that some other structural modifications of the mesophases, such as pore expansion, are driven by the Hofmann decomposition of the occluded tetraalkylammonium surfactant, yielding to the formation of the corresponding neutral hexadecyldimethylamine.[71] When this occurs, the C/N ratio decreases as the surfactant decomposition progresses. In this study, we have carried out the elemental analysis of the mesophasic samples to exclude the occurrence of Hoffman decomposition during the crystallization process. The elemental analyses, shown in Table 2, indicate that the C/N ratio is always close to 19 (within the experimental error), proving that no decomposition of the occluded hexadecyltrimethylammonium cations occurs during the course of the mesophase transformation under the synthesis conditions employed in this work.

To evaluate the phase composition of MCM-48/lamellar phase mixtures from their nitrogen adsorption isotherms and thermogravimetric weight change curves, adsorption data for pure calcined MCM-48 and calcined (collapsed) lamellar phases were required. It was of particular interest to acquire such data for pure phases synthesized under conditions similar to those used for the mixed phases to obtain pure phases of adsorption properties (adsorption capacity, specific surface area, the extent of external surface) and thermogravimetric properties similar to those for the components of mixed phases. This way of selecting the MCM-48 phase was somewhat difficult because some apparently phase-pure MCM-48 samples were found after a close examination of their XRD and adsorption data to exhibit trace amounts of the lamellar phase. However, it was possible to select an MCM-48 sample with the unit-cell size and pore diameter highly similar to those for the MCM-48 components of the mixed phases. It was also possible to find a lamellar phase, whose interplanar spacing and degree of structural ordering was similar to those for the components of the mixed phases.

XRD patterns for as-synthesized and calcined MCM-48 sample (V1), three lamellar phases (L1−L3), and four MCM-48/lamellar mixtures (VL1−VL4) are shown in Figure 1. V1 is a highly ordered MCM-48 silica, as can be seen from the well-resolved XRD pattern characteristic of *Ia*3*d* structure. The intensity of the pattern significantly increased after calcination, which is a known behavior related to the increase of contrast between the siliceous wall and the pore space[72] after the surfactant has been removed.

Table 2. Chemical Composition of the Samples

sample	C (%)	N (%)	C/N	SiO_2[a] (%)	CTA/SiO_2[b]
V1	37.81	2.29	19.3	43.45	0.229
VL1	37.29	2.27	19.2	43.50	0.226
VL2	35.91	2.18	19.2	45.46	0.208
VL3	39.38	2.39	19.2	41.37	0.251
VL4	39.34	2.38	19.3	40.13	0.258
L1	40.29	2.45	19.2	40.80	0.260
L2	42.29	2.58	19.1	39.32	0.283
L3	43.64	2.64	19.3	37.59	0.305

[a] Calculated as the residue of the thermogravimetric analysis. [b] Calculated from the carbon percentage.

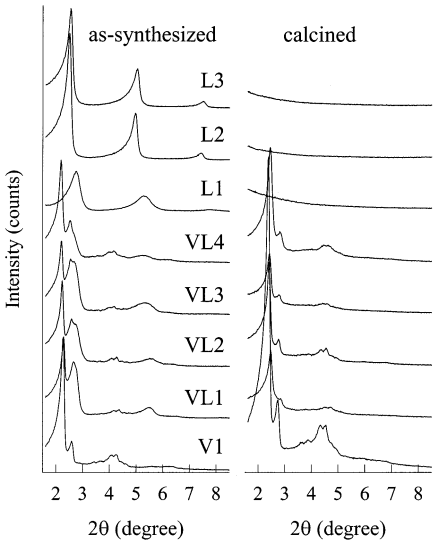

Figure 1. X-ray diffraction patterns for as-synthesized and calcined samples. The patterns for all samples except for V1 are offset vertically to allow for a better comparison.

(65) Sing, K. S. W.; Everett, D. H.; Haul, R. A. W.; Moscou, L.; Pierotti, R. A.; Rouquerol, J.; Siemieniewska, T. *Pure Appl. Chem.* **1985**, *57*, 603.
(66) Jaroniec, M.; Kruk, M.; Olivier, J. P. *Langmuir* **1999**, *15*, 5410.
(67) Kruk, M.; Jaroniec, M.; Sayari A. *Langmuir* **1997**, *13*, 6267.
(68) Landry, C. C.; Tolbert, S. H.; Gallis, K. W.; Monnier, A.; Stucky, G. D.; Norby, P.; Hanson, J. C. *Chem. Mater.* **2001**, *13*, 1600.
(69) Pevzner, S.; Regev, O. *Microporous Mesoporous Mater.* **2000**, *38*, 413.
(70) Lee, Y. S.; Surjadi, D.; Rathman, J. F. *Langmuir* **2000**, *16*, 195.
(71) Kruk, M.; Jaroniec, M.; Sayari, A. *J. Phys. Chem. B* **1999**, *103*, 4590.

Table 3. Interplanar Spacings Measured for the Samples Using X-ray Diffraction[a]

sample	d_{211}^{NC} (nm)	d_{001}^{NC} (nm)	d_{002}^{NC} (nm)	d_{211}^{C} (nm)
V1	3.91	*b*	*b*	3.71
VL1	3.86	*c*	1.61	3.58
VL2	3.96	*c*	1.59	3.67
VL3	4.02	*c*	1.66	3.65
VL4	4.03	*c*	1.68	3.59
L1	*b*	3.19	1.67	*b*
L2	*b*	3.52	1.78	*b*
L3	*b*	3.46	1.75	*b*

[a] Notation: d_{hkl}^{X}, XRD (*hkl*) interplanar spacing for the uncalcined (X = NC) and calcined (X = C) sample. [b] The corresponding XRD peak was not observed. [c] The position of the (001) peak of the lameller phase could not be accurately determined because the (001) peak overlapped with the (220) peak of the MCM-48 phase.

L1−L3 samples exhibited XRD patterns in which at least three different (0 0 *l*) basal reflections are clearly observed, indicating the lamellar structure of these materials. The XRD pattern for L1 exhibited three broad XRD reflections, whereas the patterns for L2 and L3 featured four relatively narrow peaks, indicating that the latter two samples are highly ordered as far as the stacking of layers is concerned. All peaks on XRD patterns for L1−L3 disappeared after calcination, confirming the layered nature of these materials. The XRD patterns for the other samples appeared to be superpositions of XRD patterns for the V1 MCM-48 sample and L1 lamellar phase, thus indicating that these two pure phases have unit-cell dimensions very similar to those of the components of the mixed phases. In cases of all as-synthesized mixed phases, (211), (420), and (332) peaks of MCM-48 and a broad (200) peak of the lamellar phase are visible, whereas the (220) peak of MCM-48 overlaps with the (001) peak of the lamellar phase. After the calcination, only peaks characteristic of the MCM-48 phase persisted. The d_{hkl} interplanar spacings corresponding to the main XRD reflections observed are listed in Table 3. (211) interplanar spacings for the pure MCM-48 phase and MCM-48 components of the mixed phases, whether as-synthesized or calcined, were within 0.15 nm from one another, whereas the (002) peaks of the L1 lamellar phase and lamellar components of the mixed phases were not more than 0.09 nm apart. Thus, it was possible to select pure phases that exhibited unit-cell dimensions very similar to those of the components of the mixed phases. It should be noted that the overlap between the (220) peak of the V1 MCM-48 phase and the (001) peak of the lamellar phase (which is the most prominent XRD peak for this phase) would make it difficult to perform the quantitative phase composition analysis for the mixed phases on the basis of the XRD data.

As can be seen in Figure 2, the shape of the nitrogen adsorption isotherm of V1 MCM-48 silica was very similar to adsorption isotherms for other MCM-48 silicas synthesized under different conditions, although the adsorption capacity of sample V1 was somewhat higher than the adsorption capacity for the other compared samples. It should be noted that nitrogen adsorption isotherms for MCM-48 are somewhat different from those for MCM-41 silicas. As can be seen in Figure 2 that reduced adsorption before the onset of the capillary condensation step is noticeably lower and the increase in adsorption related to the capillary condensation is larger in the case of MCM-48, when compared to MCM-41 samples that exhibit a similar capillary condensation pressure for nitrogen. These results indicate that MCM-48 silicas exhibit well-defined nitrogen adsorption properties that are noticeably different from those of MCM-41 silicas.

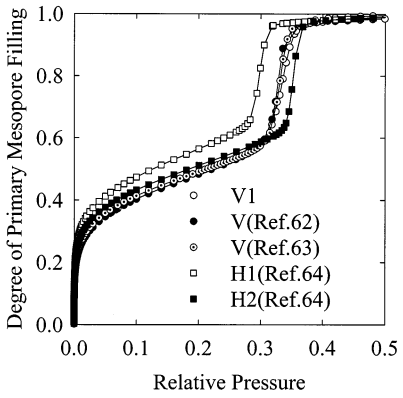

Figure 2. Comparison of degrees of primary mesopore filling for three MCM-48 silicas synthesized under different conditions (V1 is reported herein) and two MCM-41 silicas. Samples were selected to exhibit similar capillary condensation pressures.

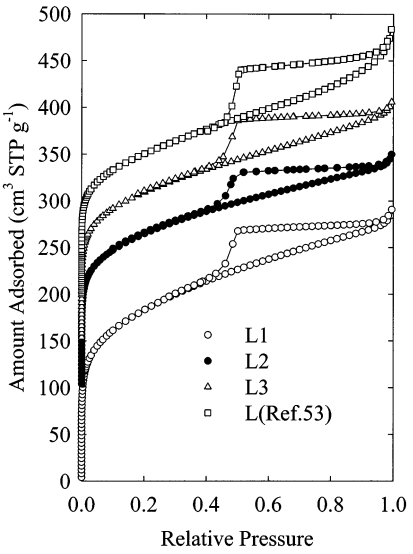

Figure 3. Nitrogen adsorption isotherms for calcined lamellar phases synthesized under different conditions (isotherms for L2, L3, and L (ref 53) are offset vertically by 100, 150, and 200 cm^3 STP g^{-1}).

Nitrogen adsorption isotherms for several calcined (collapsed) lamellar phase samples are shown in Figure 3. In contrast to the isotherms for MCM-48 and MCM-41, these isotherms did not exhibit any capillary condensation steps on the adsorption branches of isotherms, which attests to the broadness of the pore size distribution (PSD) for these disordered materials. On the other hand, there were pronounced sharp steps on the desorption branches of isotherms centered at relative pressures of about 0.45−0.50,[53] which coincides with the lower limit of the adsorption−desorption hysteresis.[63,65,73]

(72) Marler, B.; Oberhagemann, U.; Vortmann, S.; Gies, H. *Microporous Mater.* **1996**, *6*, 375.

(73) Kruk, M.; Jaroniec, M. *Chem. Mater.* **2001**, *13*, 3169.

Table 4. Structural Parameters of the Samples Calculated from Nitrogen Adsorption Data[a]

sample	S_{BET} ($m^2\ g^{-1}$)	V_t ($cm^3\ g^{-1}$)	V_p ($cm^3\ g^{-1}$)	S_{ex} ($m^2\ g^{-1}$)	V_{mi} ($cm^3\ g^{-1}$)	w_{KJS} (nm)
V1	1240	1.10	1.08	20	0.00[b]	3.7
VL1	870	0.68	0.54	70	0.02	3.5
VL2	910	0.76	0.60	90	0.02	3.7
VL3	840	0.67	0.56	50	0.03	3.6
VL4	1110	0.91	0.84	40	0.00	3.6
L1	650	0.44	0.30	50	0.06	*c*
L2	580	0.38	0.24	40	0.07	*c*
L3	560	0.39	0.23	60	0.06	*c*

[a] S_{BET}, BET specific surface area; V_t, total pore volume; V_p, primary mesopore volume; S_{ex}, external surface area; V_{mi}, micropore volume; w_{KJS}, the position of the maximum on the pore size distribution (PSD) calculated using the KJS method. [b] The α_s plot calculations provided the value of $-0.02\ cm^3\ g^{-1}$, which is unphysical, but indicates the complete lack of microporosity. [c] Very broad PSD with no prominent maximum in the mesopore range.

These sharp steps cannot be regarded as evidence of narrow PSD, and they arise from delayed capillary evaporation from the mesopore structure with narrow constrictions.[73] The shapes of adsorption isotherms for calcined lamellar phases were generally similar despite marked differences in the degree of structural ordering of these materials before calcination. The as-synthesized lamellar phase L1 and the lamellar phase L (ref 53), whose nitrogen adsorption isotherm was reported earlier in our study of MCM-41/lamellar mixtures,[53] exhibited three relatively broad XRD peaks, whereas as-synthesized L2 and L3 exhibited four narrow XRD peaks, thus suggesting the high degree of the structural ordering for the latter two samples (after calcination, all samples exhibited featureless XRD patterns). The lamellar phases discussed exhibited some variation in the extent of their specific surface area and pore volume, but no clear relation between the degree of structural ordering of the as-synthesized lamellar phases and the adsorption capacity of the calcined materials was observed (compare data in Table 4 with the data reported in ref 53). All of the calcined lamellar phases discussed were clearly microporous to an appreciable extent. It is interesting to note that calcined (collapsed) lamellar phases exhibited surprisingly high specific surface areas, which ranged from 500 to 650 $m^2\ g^{-1}$. Therefore, even MCM-48 or MCM-41 samples contaminated with appreciable amounts of the collapsed lamellar phase may exhibit very high specific surface areas, as will be shown later. Because of the fact that the lamellar phase present in the MCM-48/lamellar mixed phases considered here had a moderate degree of structural ordering, as seen from XRD, the calcined lamellar sample L1 was chosen to represent adsorption behavior of the calcined lamellar component of the mixtures.

To evaluate the phase composition of the MCM-48/lamellar mixtures from their adsorption data, an approach analogous to that reported earlier for MCM-41/lamellar phase mixtures[53] was employed. The nitrogen adsorption isotherm for a given mixed phase sample, $v_{VL}(p/p_0)$, was fitted with a linear combination of the nitrogen adsorption isotherms for pure MCM-48 silica, $v_V(p/p_0)$, and pure calcined lamellar phase, $v_L(p/p_0)$,

$$v_{VL}(p/p_0) \text{ fitted with } x_c^{Ai}(V)v_V(p/p_0) + x_c^{Ai}(L)v_L(p/p_0) \quad (1)$$

where $x_c^{Ai}(V)$ and $x_c^{Ai}(L)$ are fitting coefficients and V stands for cubic MCM-48 phase and L stands for lamellar phase. The pure MCM-48 and lamellar phases were represented by V1 and L1 samples, respectively. The subscript "c" indicates that the fitting coefficients reflect the weight fractions of the calcined samples, whereas the superscript "A*i*" indicates that the coefficients were determined from adsorption data using one of two fitting procedures. In the first method ("A1"), the sum of fitting coefficients was set to be equal to 1 (that is, 100%). In the second procedure ("A2"), no restrictions on the values of the fitting coefficients were introduced. As the fitting coefficients reflect weight fractions of the pure phases in the mixture, the sum of the fitting coefficients is expected to be equal to 1 (unless there is an additional phase, such as non-mesostructured amorphous silica, present). However, this expectation is based on the assumption that the adsorption capacities of the particular components of the mixed phases are exactly the same as those for the corresponding pure phases. Moreover, this assumption does not take into account the possibility that experimental errors in adsorption measurements may amount to several percent. Therefore, it is not required to force the sum of the fitting coefficients to be exactly equal to 1. On the other hand, when the sum of fitting coefficients assumes the value of 1 (100%) or close to 1 and the quality of fit is high, one can expect that the pure phases used to represent the components of the mixture were selected very well and, more importantly, that the fitting coefficients can be regarded as exact contents of the particular phases in the mixture. It also should be noted that the fitting was carried out using adsorption branches of isotherms only and that the data in the capillary condensation region (relative pressure range from 0.25 to 0.4) were omitted.[53] The latter omission was made to eliminate an error in fitting that might arise from the slight difference in the position of the capillary condensation steps for the pure MCM-48 and the MCM-48/lamellar mixture under study.

Very good fits were obtained for the entire adsorption branches of the isotherms, including the low-pressure region (see Figures 4 and 5), and the sums of fitting coefficients were remarkably close to 100% (that is, 1) (see Table 5), when the fitting procedure without restrictions on the values of the fitting coefficients was employed. Therefore, the fitting coefficients can be regarded as weight fractions of particular phases in the mixed phases. On the basis of these data, one can conclude that, among the mixed phases, only sample VL4 exhibited more than 50% of the MCM-48 phase, whereas the other three samples had only 30−50% of the MCM-48 phase. This conclusion is by no means obvious because all these phases had very high nitrogen BET specific surface areas of 800−1100 $m^2\ g^{-1}$ and high pore volumes (Table 4), although the very occurrence of the contamination with the calcined lamellar phase was clear from the presence of a triangular hysteresis loop at relative pressures from 0.4 to 1 on the adsorption isotherms. Indications about the presence of the contamination in the MCM-48/lamellar samples considered can be obtained from the α_s plot method, which indicates no microporosity for pure MCM-41 sample and slight microporosity for most of the mixed phases (see Table

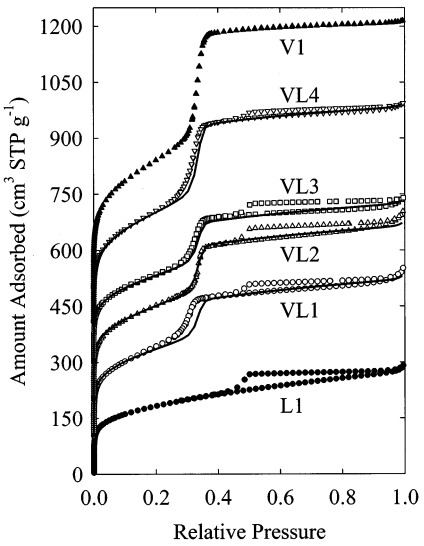

Figure 4. Nitrogen adsorption isotherms for calcined samples: pure MCM-48 (V1), pure lamellar phase (L1), and four MCM-48/lamellar mixtures. Symbols denote experimental data points, whereas lines show fits of the isotherms for mixed phases with linear combinations of adsorption isotherms for pure phases. No restrictions on values of fitting coefficients were introduced. The isotherms for VL1, VL2, VL3, VL4, and V1) and corresponding fits are offset vertically by 100, 200, 300, 400, and 500 cm^3 STP g^{-1}, respectively.

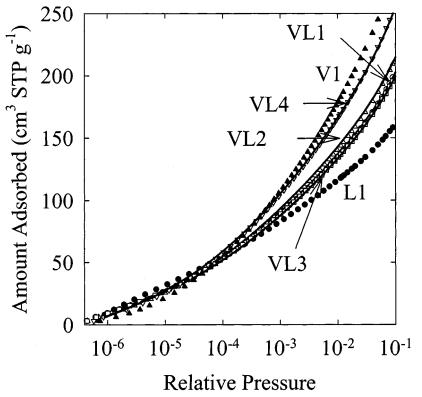

Figure 5. Low-pressure parts of nitrogen adsorption isotherms for calcined pure MCM-48, pure lamellar phase, and MCM-48/lamellar mixtures. Symbols denote experimental data points, whereas lines show fits of the isotherms for mixed phases with linear combinations of adsorption isotherms for pure phases.

4). In particular, the low-pressure part of the α_s plot exhibited good linearity for MCM-48, and in this case, the line drawn through the α_s interval from 0.4 to 0.7 intercepted the "Amount Adsorbed" axis slightly below 0, whereas the intercepts for the MCM-48/lamellar mixtures were somewhat above 0 (see Figure 6). The calcined (collapsed) lamellar phase is microporous to an appreciable extent (see Table 4 and ref 53), as seen from the significant positive value of the intercept (see Figure 6). So the α_s plot analysis provides some information about the contamination of MCM-48 samples with the collapsed lamellar phase. However, to quantify the extent of this contamination, a more elaborated method needs to be employed. In the method proposed here, the quality of the fit can be used to judge whether the data for the pure components used for the fitting procedure are adequate or not. A poor fit would indicate that the

Table 5. Estimated Phase Composition of the MCM-48/Lamellar Mixtures[a]

sample	x_c^{A1}(V) (%)	x_c^{A1}(L) (%)	x_c^{A2}(V) (%)	x_c^{A2}(L) (%)	$x_n^{TGA,Y}$(L) (%)	$x_n^{TGA,P}$(L) (%)
VL1	34	66	34	66	50	59
VL2	44	56	44	56	43	32
VL3	35	65	38	57	59	67
VL4	71	29	66	42	36	38

[a] Notation: $x(A)$, weight fraction of component A in the mixture (A = V for MCM-48 and A = L for lamellar phase); subscripts "c" and "n" denote calcined and uncalcined (as-synthesized) samples, respectively; superscripts "A1"and "A2" denote the estimates based on nitrogen adsorption data, which were obtained using a procedure with no restrictions on the values of the fitting coefficients ("A2") or under assumption that the sum of the fitting coefficients is equal to 1 (that is, 100%) ("A1"); superscripts "TGA,Y" and "TGA,P" denote estimates obtained from TGA data on the basis of the low-temperature weight loss peak height ("TGA,Y") and the weight loss between 373 and 423 K.

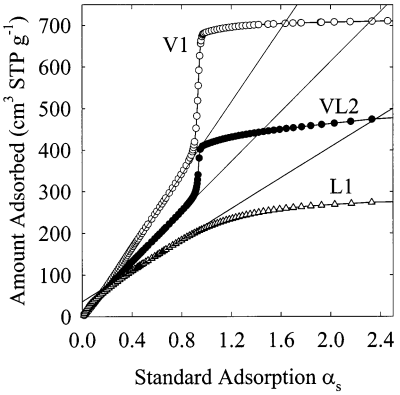

Figure 6. α_s plots for selected calcined samples.

mixture contains components of adsorption properties (and thus structures) different from those assumed. Large deviations of the sum of the fitting coefficients from 100% would usually indicate that the components of the mixed phase have different adsorption capacities than those for the pure components used for the analysis, although large negative deviations would point to the presence of an additional low-surface-area amorphous phase.

As demonstrated earlier for MCM-41/lamellar mixtures, the phase composition analysis can also be achieved on the basis of thermogravimetric weight change curves for as-synthesized materials.[53] This was possible because of the prominent difference in the weight loss behavior for as-synthesized MCM-41 and lamellar phase, as the latter starts to decompose at much lower temperature. It has been reported earlier[63] that as-synthesized MCM-48 exhibits weight change patterns similar to those observed for MCM-41 templated by the same surfactant. Therefore, it could be expected that the thermogravimetric analysis of the phase composition of MCM-48/lamellar mixtures is feasible. This study demonstrated that this is indeed the case. Shown in Figure 7 are weight change derivatives for the as-synthesized pure MCM-48, pure lamellar phase, and the four mixed phases under study. It can be seen that the pure lamellar phase and the samples containing some amount of this phase exhibited a prominent weight loss event at around 410 K, whereas there was no significant weight loss for MCM-48 at this temperature. This behavior paralleled that observed for

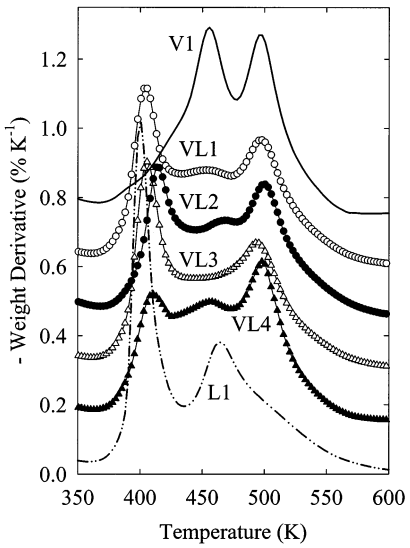

Figure 7. Weight change derivatives for as-synthesized samples.

as-synthesized MCM-41/lamellar mixtures. The height of the peak at about 410 K on the weight change derivative can be used to estimate the lamellar phase content by simply dividing the height of this peak for the mixed phase by the height of this peak for the pure lamellar phase. Thus-obtained estimates of the content of the lamellar phase are listed in Table 5 (with superscript "TGA,Y"). It is notable that the height of the considered low-temperature peak is generally similar to those of the lamellar phases synthesized under different conditions (samples L1−L3 and L (ref 53)) in the presence of hexadecyltrimethylammonium surfactant. However, this similarity was observed in the case where TGA runs were carried out in the same mode and atmosphere, and using approximately the same sample weight, whereas even the change of the sample size led to some changes of the peak height. Therefore, before the use of the TGA-based method is attempted, one needs to ascertain that the TGA data can be acquired with acceptable reproducibility.

In the earlier study of MCM-41/lamellar mixtures, it was possible to evaluate the content of the lamellar phase on the basis of the weight loss between temperatures of certain minima on the weight change derivatives.[53] This approach allowed one to improve the reproducibility of the phase composition estimates from TGA data. However, in the case of the aforementioned study, the weight change curves for mixed phases were superpositions of the ones for the pure phases. The visual inspection of the TGA data reported herein shows that this is not the case because the MCM-48 component of the mixed phases appears to exhibit a predominant weight loss centered at about 500 K, whereas pure MCM-48 exhibited major weight loss events at both 450 and 500 K. Because of these differences in the weight change behavior between the pure MCM-48 and the MCM-48 component of the mixed phases, the calculation procedure based on the weight loss in certain temperature ranges had to be modified. It was observed that the weight loss between 373 and 423 K for MCM-48 was rather small (about 5%) and did not vary much from one sample to another. This observation allows one to use weight loss in this range to estimate the content of the lamellar phase in the following way. The weight loss observed between 373 and 423 K for the lamellar phase L1 was about 21% (the weight losses for the other, better ordered lamellar phases L2 and L3 were very similar). Under assumptions that as-synthesized MCM-48 and lamellar components of the MCM-48/lamellar mixture exhibit weight losses of 5 and 21%, respectively, in the temperature range from 373 to 423 K and that the sum of phase contents of MCM-48 and lamellar phases is 1 (i.e., 100%), one can estimate the phase composition. The corresponding estimates for the lamellar phase contents are listed in Table 5 (denoted with superscript "TGA,P").

Additionally, it was observed that the CTA/SiO_2 ratio (Table 2) roughly increased as the percentage of lamellar phase in the material increased. Indeed, it is observed that the pure MCM-48 sample yields to a CTA/SiO_2 ratio of 0.23 that constantly increases up to values close to 0.29 for the lamellar compounds. The exception of sample VL2 can be understood by considering the synthesis conditions of this particular sample, which was obtained at lower temperature and longer crystallization time than the other materials studied in this work.

In most cases, the estimation of the lamellar phase percentage based on TGA data was similar to those from nitrogen adsorption data and roughly correlate with the content of occluded surfactant. However, because of some irreproducibility in TGA measurements, and the lack of the possibility to verify the self-consistency of results obtained from TGA, it is expected that the results derived from nitrogen adsorption data are more accurate. In addition, the TGA-based method may not be particularly suitable for heteroatom-incorporated MCM-48/lamellar silicates because the presence of heteroatoms may influence the surfactant decomposition process and thus influence the weight loss behavior.[74] On the other hand, the presence of heteroatoms in silica-based frameworks is not known to have any major impact on the nitrogen adsorption behavior,[75] and thus the adsorption-based method for the quantitative phase composition assessment is expected to be well suited for heteroatom-incorporated mixed-phase silicates.

Conclusions

Nitrogen adsorption and thermogravimetry can be readily used to quantify the contents of MCM-48 and lamellar phases in the MCM-48/lamellar mixed phases. Quantitative analysis based on gas adsorption data is possible because of the striking differences in the adsorption behavior between MCM-48 and calcined lamellar phase and the general similarity in the adsorption behavior of different MCM-48 samples with similar pore diameters as well as different calcined lamellar phases synthesized under different conditions. However, the availability of pure phases with structural properties highly similar to those of the components of mixed phases greatly facilitates the quantitative analysis. The adsorption isotherms for MCM-48/lamellar mixed phases can be described as a linear combination of the adsorp-

(74) Schmidt, R.; Akporiaye, D.; Stocker, M.; Ellestad, O. H. *Stud. Surf. Sci. Catal.* **1994**, *84*, 61.
(75) Kruk, M.; Jaroniec, M.; Sayari, A. *Langmuir* **1999**, *15*, 5683.

tion isotherms for pure components and the fitting coefficients can be regarded as the estimates of the weight fractions of pure phases in the mixtures. Although there are clear differences in nitrogen adsorption behavior of pure MCM-48 and MCM-41, these differences are so small that the determination of the phase composition of MCM-48/MCM-41 mixtures from gas adsorption isotherms is likely to be highly inaccurate. The semiquantitative determination of the phase composition of MCM-48/lamellar phase mixtures can also be carried out on the basis of the weight change curves for as-synthesized samples because of the differences in the surfactant decomposition temperatures for as-synthesized MCM-48 and the lamellar phase. The obtained results are similar to those obtained from gas adsorption data. However, it will need to be verified if the quantification by TGA can be achieved in the case of heteroatom-incorporated MCM-48 silicas as the presence of heteroatoms may significantly alter the surfactant thermal decomposition pattern. However, it is known that the presence of heteroatoms in silica-based frameworks does not change the nitrogen adsorption behavior to any significant extent and thus the accuracy and reliability of the quantitative phase analysis from adsorption data should not be affected by the presence of heteroatoms.

Acknowledgment. The donors of the Petroleum Research Fund administered by the American Chemical Society are gratefully acknowledged for the support of this research. F.R. and M.L.P thank the Spanish CICYT (MAT 2000-1167-C02-01 Project) for financial support.

CM020616I